

# Dynamic Sequential Layer-by-Layer Deposition Method for Fast and Region-Selective Multilayer Thin Film Fabrication

Hyong-Jun Kim,<sup>†</sup> Kangwon Lee,<sup>†</sup> Sameer Kumar,<sup>†</sup> and Jinsang Kim<sup>\*,†,‡</sup>

Department of Materials Science and Engineering, Chemical Engineering, Macromolecular Science and Engineering, and Biomedical Engineering, University of Michigan, Ann Arbor, Michigan 48109

Received April 26, 2005. In Final Form: June 14, 2005

We present a newly devised technique, the dynamic layer-by-layer (LbL) deposition method, that is designed to take advantage of the LbL deposition method and fluidic devices. Polyelectrolyte solutions are sequentially injected through the fluidic LbL deposition device to quickly build well-defined multilayer films on a selected region with a linear increase in the material deposited. Multilayer film fabrication by this new method on a specific region was proven to be fast and effective. The effects on film quality of the processing parameters such as concentration of polyelectrolytes, flow rate, and contact time were investigated. A half-tethered self-standing film on a substrate was fabricated to demonstrate the effectiveness and the region-selective deposition capability of the devised dynamic LbL deposition method.

## Introduction

Molecular assembly methods have been an exciting subject for the past several decades for the fabrication of functional materials such as nanocrystals and polymers into organized films at the molecular level. One of the most recent molecular assembly techniques is the alternating adsorption of oppositely charged polyelectrolytes, the “layer-by-layer (LbL)” self-assembly method. Although studies of self-assembly by alternating adsorption of oppositely charged polyions were reported in 1960s,<sup>1</sup> a practical method was only developed in the early 1990s by Decher et al.<sup>2,3</sup> This particular technique has garnered strong interest in the past decade due to its simplicity. The method is also versatile because not only polyelectrolytes but also charged nanoobjects, such as molecular aggregates,<sup>4</sup> clusters,<sup>5</sup> or colloids,<sup>6</sup> can be used.

Various studies have been performed, for example, the characterization of LbL multilayer films by using X-ray<sup>7</sup> or neutron reflectivity<sup>8</sup> and control of the film thickness by adding salts<sup>9,10</sup> or by changing the pH<sup>11–13</sup> of the solution. These variations change the surface morphology and consequently the film characteristics such as refractivity,<sup>12</sup> wettability,<sup>13</sup> and mechanical strength.<sup>14,15</sup> How-

ever, the conventional LbL multilayer fabrication technique is a time-consuming equilibrium process and lacks region-selective deposition capability. The conventional LbL method also cannot provide in-plane alignment of adsorbed polyelectrolytes, which will have many applications.

The need for faster processes has given birth to a few modified techniques. These techniques include the combination of the LbL principle with the capillary force inside microchannels,<sup>16</sup> spin casting,<sup>17</sup> or spraying<sup>18</sup> to produce similar quality multilayer films in a much shorter processing time. Very recently, several region-selective deposition procedures also have been developed by combining the conventional LbL deposition with chemical patterning of a substrate<sup>19,20</sup> or microcontact printing.<sup>21–23</sup>

Here, we report a new multilayer film fabrication method that combines the advantages of the LbL film deposition, soft lithography technique, and fluidic device design so that well-defined multilayer polymeric films can be quickly and easily fabricated on a specific target area of a substrate. Multilayer films can be fabricated in 90 s of processing time, and the resulting films have a similar quality in terms of film thickness and roughness compared to those fabricated by the conventional LbL dipping method. The effects of the processing parameters such as the concentration of polyelectrolytes, flow rate, and contact time on the film quality were systematically studied. A half-tethered self-standing film on a substrate was fabricated to demonstrate the effectiveness and the region-selective deposition capability of the devised dynamic LbL deposition method.

This new method could be widely applicable for molecular manipulations of functional nano-objects,<sup>24,25</sup> other polyelectrolytes, and biomolecules.<sup>26,27</sup> There are also po-

\* To whom correspondence should be addressed. E-mail: jinsang@umich.edu.

<sup>†</sup> Department of Materials Science and Engineering.

<sup>‡</sup> Chemical Engineering, Macromolecular Science and Engineering, and Biomedical Engineering.

(1) Iler, R. K. *J. Colloid Interface Sci.* **1966**, *21*, 569.

(2) Decher, G.; Hong, J.-D. *Makromol. Chem., Macromol. Symp.* **1991**, *46*, 321.

(3) Decher, G. *Science* **1997**, *277*, 1232.

(4) Kramer, G.; Buchhammer, H.-M.; Lunckwitz, K. *Colloids Surf. A* **1995**, *122*, 1.

(5) Schmitt, J.; Decher, G.; Dressick, W. J.; Brandow, S. L.; Geer, R. E.; Shashidhar, R.; Calvert, J. M. *Adv. Mater.* **1997**, *9*, 61.

(6) Krozer, A.; Nordin, S.-A.; Kasemo, B. *J. Colloid Interface Sci.* **1995**, *176*, 479.

(7) Lvov, Y.; Decher, G.; Möhwald, H. *Langmuir* **1993**, *9*, 481.

(8) Kellog, G. J.; Mayes, A. M.; Stockton, W. B.; Ferreira, M.; Rubner, M. F.; Satija, S. K. *Langmuir* **1996**, *12*, 5109.

(9) Dubas, S. T.; Schlenoff, J. B. *Macromolecules* **1999**, *32*, 8153.

(10) Tsukruk, V. V.; Bliznyuk, V. N.; Visser, D. A.; Campbell, L.; Bunning, T. J.; Adams, W. W. *Macromolecules* **1997**, *30*, 6615.

(11) Yoo, D.; Shiratori, S. S.; Rubner, M. F. *Macromolecules* **1998**, *31*, 4309.

(12) Hiller, J.; Mendelsohn, J. D.; Rubner, M. F. *Nat. Mater.* **2002**, *1*, 59.

(13) Zhai, L.; Cebeci, F. C.; Cohen, R. E.; Rubner, M. F. *Nano Lett.* **2004**, *4*, 1349.

(14) Hua, F.; Cui, T.; Lvov, Y. M. *Nano Lett.* **2004**, *4*, 823.

(15) Jiang, C.; Markutsya, S.; Pikus, Y.; Tsukruk, V. V. *Nat. Mater.* **2004**, *3*, 721.

(16) Jang, H.; Kim, S.; Char, K. *Langmuir* **2003**, *19*, 3094.

(17) Cho, J.; Char, K.; Hong, J.-D.; Lee, K.-B. *Adv. Mater.* **2001**, *13*, 1076.

(18) Porcel, C. H.; Izquierdo, A.; Ball, V.; Decher, G.; Vögel, J.-C.; Schaaf, P. *Langmuir* **2005**, *21*, 800.

(19) Clark, S. L.; Hammond, P. T. *Langmuir* **2000**, *16*, 10206.

(20) Jiang, X.-P.; Clark, S. L.; Hammond, P. T. *Adv. Mater.* **2001**, *13*, 1669.

(21) Park, J.; Hammond, P. T. *Adv. Mater.* **2004**, *16*, 520.

(22) Zhou, D.; Bruckbauer, A.; Batchelor, M.; Kang, D.-J.; Abell, C.; Klenerman, D. *Langmuir* **2004**, *20*, 9089.

(23) Kohli, N.; Worden, R. M.; Lee, I. *Chem. Comm.* **2005**, 316.

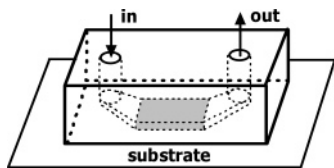


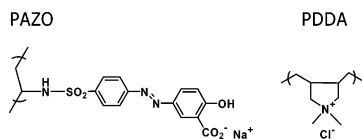
**Figure 1.** Fluidic device used to deposit polyelectrolytes on substrates. The open section (the shaded area) at the bottom of the device has a dimension of  $20 \times 10 \times 2$  (length  $\times$  width  $\times$  height)  $\text{mm}^3$ .

tential advantages of this method, for example, shear-induced alignment of rodlike conjugated polymers which is currently under investigation as an extension of this report.

### Experimental Section

**Materials.** Poly(diallyldimethylammonium chloride) (PDMA) (MW = 100 000–200 000) and poly(1-4-(3-carboxy-4-hydroxyphenylazo)benzene sulfonamido)-1,2-ethandiyl, sodium salt (PAZO) were purchased from Aldrich. Aqueous solutions of the polymers were prepared in  $18\text{M}\Omega$  deionized water. The molar concentration was calculated based on the repeat unit of each polyelectrolyte that is shown in the Scheme 1. Silicon wafers and glass slides were cleaned in  $\text{NH}_4\text{OH}/\text{H}_2\text{O}_2/\text{H}_2\text{O}$  1:1:4 solution for 30 min at  $80^\circ\text{C}$  followed by immersion in  $\text{H}_2\text{SO}_4/\text{H}_2\text{O}$  7:3 solution for 1 h. [Caution: These solutions are highly corrosive.] The cleaned substrates were pre-deposited with 1 mM PDMA solution for 10 min, and the resulting positively charged substrates were used immediately.

#### Scheme 1. Chemical Structure of PAZO and PDMA



**Device Fabrication and Dynamic LbL.** The fluidic device was made with poly(dimethylsiloxane) (PDMS, Dow Corning Sylgard 184) to have a flow geometry shown in Figure 1. A flow channel with a rectangular deposition area was chosen. However, the dimension of the deposition area can be designed to be any size depending on the needs. The two vertical holes were connected to plastic tubes that were linked to a syringe pump. First, a 2-mm-thick aluminum plate was cut into the desired shape and placed into a mold. Premix of PDMS and a cross-linking agent (supplied with Sylgard 184, 10/1 w/w) was poured into the mold. Entrapped air was removed by vacuum, and the PDMS was cured at  $100^\circ\text{C}$  for 2 h. After the curing the aluminum plate was removed to make the fluidic device depicted in Figure 1. Because PDMS tends to uptake dusts in air, caution should be taken not to contaminate the flow channel and the contact area. The fluidic device can be located anywhere on a glass substrate to form a leak-free flow channel, allowing region-selective deposition.

The LbL deposition of polyelectrolytes was done by injecting polymer solution through the flow channel from a 20 mL syringe using a Sage syringe pump. The average flow rate at the deposition region was set at 1 cm/s. The deposition sequence started with injecting PAZO solution, water, PDMA solution, and water into the channel up to a certain number of layers. The outermost polyelectrolyte layer was always PAZO. The leftover solution in the fluidic device was drained after each injection, and the next injection was begun immediately after washing the flow channel with the deionized water at the flow rate of 1 cm/s.

(24) Huang, Y.; Duan, X.; Wei, Q.; Lieber, C. M. *Science* **2001**, *291*, 630.

(25) Guldi, D. M.; Mamedov, A.; Crisp, T.; Kotov, N. A.; Hirsch, A.; Prato, M. *J. Phys. Chem. B* **2004**, *108*, 8770.

(26) Reyes, D.; Perruccio, E. M.; Becerra, P.; Locascio, L. E.; Gaitan, M. *Langmuir* **2004**, *20*, 8805.

(27) Vasina, E. N.; Dejaridin, P. *Langmuir* **2004**, *20*, 8699.

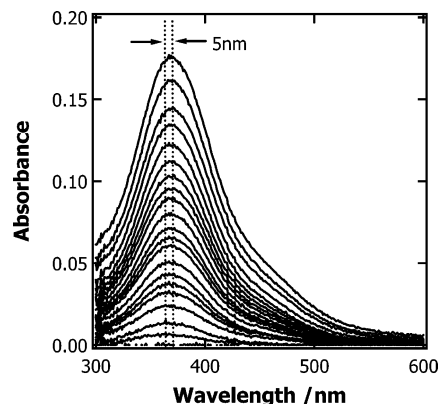


**Figure 2.** UV/Vis spectra of 1 mM/10 mM PAZO/PDDA multilayer films prepared by the dynamic LbL deposition device. Polyelectrolyte solutions and deionized water were injected sequentially through the fluidic device at a flow rate of 1 cm/s for a contact time of 90 s. The deposition sequence was PDMA–water–PAZO–water. Scans were performed every 2-bilayer of deposition.

All the solutions were changed after at most 10-bilayer deposition cycles. As the concentration of PDMA increases, the deposition solution should be changed more frequently due to the salt exchange during the multilayer buildup.<sup>9</sup> For example, solutions were changed every four bilayers deposited using 100 mM PDMA. Multilayer films were fabricated up to 40-bilayer on glass slides measuring UV/Vis absorption after each bilayer. 20-bilayer was deposited on silicon wafers to observe film thickness and surface morphology.

**Measurements.** UV/Vis absorption spectra were recorded with a Varian Cary50 UV/Vis spectrophotometer. Film thickness was measured using an ellipsometer (Rudolph Auto EL ellipsometer). Ellipsometry was performed using a HeNe laser (collimated beam of elliptically polarized light) at 632.8 nm with an incidence angle of  $70^\circ$ . The surface of the resulting polymer films was analyzed by tapping mode Atomic Force microscopy (AFM, DI Instruments Nanoscope III).

### Results and Discussion

**Dynamic LbL Deposition.** Figure 2 clearly shows the linearly increasing UV/Vis spectra of multilayer films (up to 40-bilayer) that were prepared by sequential injection of 1 mM/10 mM PAZO/PDDA solutions through the dynamic LbL deposition device. Each spectrum represents a scan after two further bilayers were deposited, the outermost layer being PAZO. The absorption at 366 nm is due to the  $\pi$ - $\pi^*$  transition of the *trans*-azobenzene moiety of PAZO,<sup>28</sup> and the red-shift by 5 nm for the first 10-bilayer suggests an aggregate formation.<sup>29</sup> No further red shift was observed in the UV/Vis spectra after 10-bilayer deposition. A similar trend of absorption shifts has been reported in PAZO/PEI (polyethyleneimine) films fabricated by the conventional LbL method.<sup>30,31</sup>

Figure 3A shows the relation between the UV absorption intensity at  $\lambda_{\text{max}} \sim 366$  nm of the multilayer films and the number of bilayers deposited. The multilayer film deposition shows linear growth. As observed by Dante et al. in a PDMA/PAZO system,<sup>30</sup> there is a slight slope change at around 20-bilayer. Similar slope changes have been

(28) Rau, H. *Photoisomerization of Azobenzenes in Photochemistry and Photophysics*; Rabek, J. F., Eds.; CRC Press: Boca Raton, FL, 1990; Vol. II, pp 119–141.

(29) Kuhn, H.; Möbius, D.; Bücher, H. *Spectroscopy of Monolayer Assemblies in Techniques of Chemistry*; Weissberger, A., Rossiter, B. W., Eds.; Wiley: New York, 1972; Vol. 1, Part 3b, pp 577–702.

(30) Dante, S.; Advincula, R.; Frank, C. W.; Stroeve, P. *Langmuir* **1999**, *15*, 193.

(31) Chiarelli, P. A.; Johal, M. S.; Holmes, D. J.; Casson, J. L.; Robinson, J. M.; Wang, H.-L. *Langmuir* **2002**, *18*, 168.

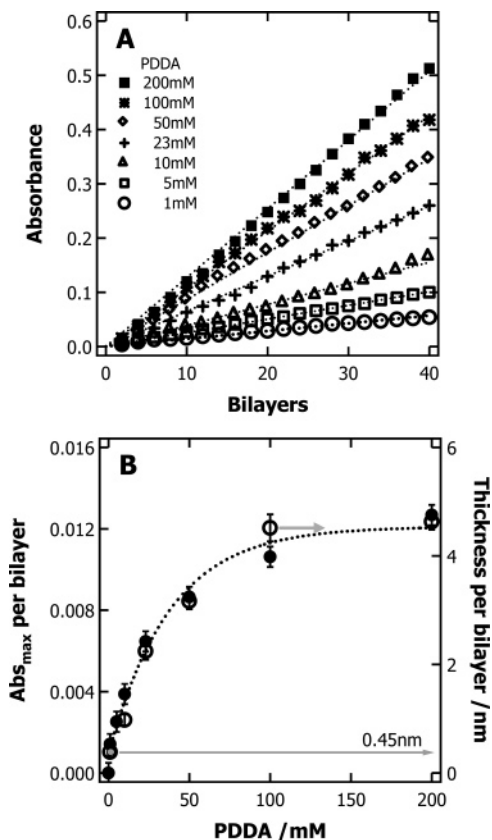


**Figure 3.** (A) UV/Vis absorbance at  $\lambda_{\max}$  ( $\sim 366$  nm) at every 2-bilayer deposition. Sequential deposition was conducted with 1 mM PAZO and PDDA aqueous solution of 1 (O), 5 (□), 10 (△), 23 (+), 50 (◇), 100 (\*), and 200 mM (■). (B) Average absorbance (●) and thickness (○) were plotted as a function of PDDA concentration. Broken lines are guides for the eye. Flow rates of the polymer solutions and the deionized water were set at 1 cm/s, and contact times were 90 s.

observed in PAZO/PEI and PAA (polyacrylic acid)/PDDA systems<sup>31</sup> where the slope of the PAZO/PEI system decreased while that of the PAA/PDDA increased even though the film thickness per bilayer remained at a constant during deposition in both cases.<sup>30,31</sup> The authors concluded that the decreased UV absorbance does not mean a decrease of the transferred PAZO polymer but is likely due to a development of disorder in the azo groups in the highly stacked multilayer films. In our case, the slope change of the UV/Vis intensity at 20-bilayer is minimal, suggesting that the resulting shear-driven multilayer film is more organized in the normal to the plane direction than in films from the conventional LbL method.<sup>30</sup>

Figure 3B shows the UV/Vis maxima and the measured film thickness by ellipsometry as the PDDA concentration increases. The measured film thickness and the UV/Vis absorption maxima are almost perfectly consistent with each other. This indicates that the dynamic LbL deposition method produces a well-organized film since there is no mismatch between the UV/Vis absorption maxima and the measured film thickness that has been observed in the multilayer films prepared by using the conventional LbL dipping method.<sup>30,31</sup>

The bilayer thickness of the deposited films prepared with 1 mM/1 mM PAZO/PDDA has almost the same value of 0.45 nm with that of the film obtained by using the conventional LbL method,<sup>30</sup> suggesting that the bilayer thickness by using this dynamic LbL method is possibly one molecule thick.

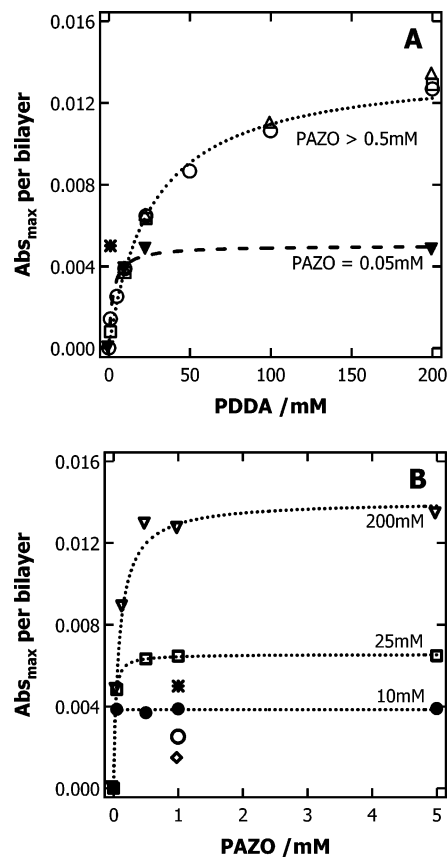


**Figure 4.** Average absorption maxima ( $\lambda_{\max} \sim 366$  nm) per bilayer deposition as PDDA and PAZO concentration changes. (A) The average UV absorption intensity is plotted as a function of PDDA concentration with PAZO concentration of 0.05 (▼), 0.5 (□), 1 (○), and 5 mM (△). (B) The average absorption maxima are plotted vs PAZO concentration with PDDA concentration of 1 (◇), 5 (○), 10 (●), 25 (□), and 200 mM (▽). Reference value from Dante et al.<sup>30</sup> (\*) is shown for comparison. All the flow rates were set at 1 cm/s, and contact times were 90 s. Lines are fitted to the data with the Langmuir isotherm.

**Concentration Effects.** Several studies on the concentration effect of LbL deposition were reported.<sup>32,33</sup> Raposo et al. studied the adsorption process of poly(*o*-methoxyaniline) and reported that the amount of adsorbed polyelectrolyte was proportional to the concentration while longer time was taken to reach its equilibrium saturation condition.<sup>32</sup> Cho et al. investigated the spin-on LbL process and found that the increase of solution concentration tends to produce a thicker adsorbed polymer layer due to increased viscosity and electrostatic forces.<sup>33</sup>

To investigate the adsorption behavior of polyelectrolytes in our dynamic LbL deposition method, we used various concentrations of polyelectrolyte solutions. The film thickness measured by ellipsometry is consistent with the UV/Vis absorption intensity. Therefore, hereafter we will interpret UV absorption intensity as the amount of adsorbed polymer. Figures 4A,B show the relation between the amount of adsorbed polyelectrolytes and the concentration of PDDA and PAZO, respectively. The reported UV/Vis values from the conventional LBL method are 2 times higher using the same 1 mM/1 mM PAZO/PDDA system, while the thickness per bilayer has the same value of 0.45 nm reported by Dante et al. (almost a monomo-

(32) Raposo, M.; Oliveira, O. N. *Langmuir* **2002**, *18*, 6866.

(33) Cho, J.; Lee, S.-H.; Kang, H.; Char, K.; Koo, J.; Seung, B. H.; Lee, K.-B. *Polymer* **2003**, *44*, 5455.

lecular thickness).<sup>30</sup> The smaller UV/Vis absorption from the same thickness likely means that the density of our dynamic LbL film is lower than that of those from the conventional LbL method. We postulate that this is caused by less effective interdigitation between polyelectrolytes in our dynamic LbL system, which is expected considering the shear force at the surface. Decher suggested the presence of interlayer diffusion or interdigitation in the conventional LbL multilayer films after analyzing the neutron reflectivity data<sup>3</sup> and the AFM images of the LbL multilayer films that showed many corrugate agglomerates with a roughness ranging from several angstroms to a few nanometers.<sup>7,17,34–36</sup> In addition, Bragg peaks implying well-defined multilayer structures are not usually observed in conventional LbL multilayer films by X-ray reflectivity.<sup>3,7,8</sup> This suggests that the multilayer films built by the LbL method usually do not consist of discrete layers. Instead, the multilayers have interdigitated structures as suggested by Decher.<sup>3</sup> Despite this interdigitation of the polyelectrolytes, the layer thickness is known to be considerably smaller than the radius of gyration of the polyelectrolytes.<sup>10</sup>

Roughness of multilayer films is an important parameter in defining the film quality. Roughness of LbL films is close to that of the substrate for the first layer and generally increases with the increasing number of layers.<sup>8,36</sup> Figure 5 shows surface topology examined with AFM of the 20-bilayer films built by the conventional LbL method (A, B) and by our dynamic deposition method (C, D, E, and F). AFM roughness measurements of the multilayer films fabricated with the same 1 mM/1 mM PAZO/PDDA aqueous solutions gave 1.5 nm by the conventional dipping method for a 30 min dipping time (B) and 2.2 nm by our dynamic sequential deposition for a 90 s contact time (C). These numbers are within the reported roughness range of conventional LbL multilayer films fabricated in equilibrium conditions.<sup>7,17,34–36</sup> However, the surfaces of the multilayer films (A) fabricated with the same 1 mM/1 mM PAZO/PDDA aqueous solutions by the conventional dipping method for the same 90 s dipping time are rougher than C. The rms roughness was 2.6 nm larger than the 2.2 of the films from the dynamic LbL deposition method. This suggests that our dynamic LbL sequential deposition method produces smooth films even though the adsorption time of our method is 90 s.<sup>7,8,17,34–36</sup> External shear force is believed to flatten the surface, making the deposited film smooth similar to a centrifugal force that induces a smoother film from the spin-on LbL deposition by pressing the LbL film downward.<sup>17</sup> The observed domains in Figure 5C have essentially the same magnitude as those in Figure 5B. As the concentration increased, the mean domain size increased from 12 nm (C) to 250 nm (F), and its distribution increased.

The overall film thickness and roughness increased as the polyelectrolyte concentration increased as shown in Figure 5G. We believe that as the polyelectrolyte concentration increases polyelectrolytes have more intermolecular chain entanglement, resulting in larger film roughness as well as a thicker film. This concentration effect on the intermolecular chain entanglement of polyelectrolytes is similar to the pH and salt effects on the intramolecular chain conformation of polyelectrolytes in the conventional LbL method and eventually influences the resulting film thickness and roughness.<sup>9,10</sup> In the con-

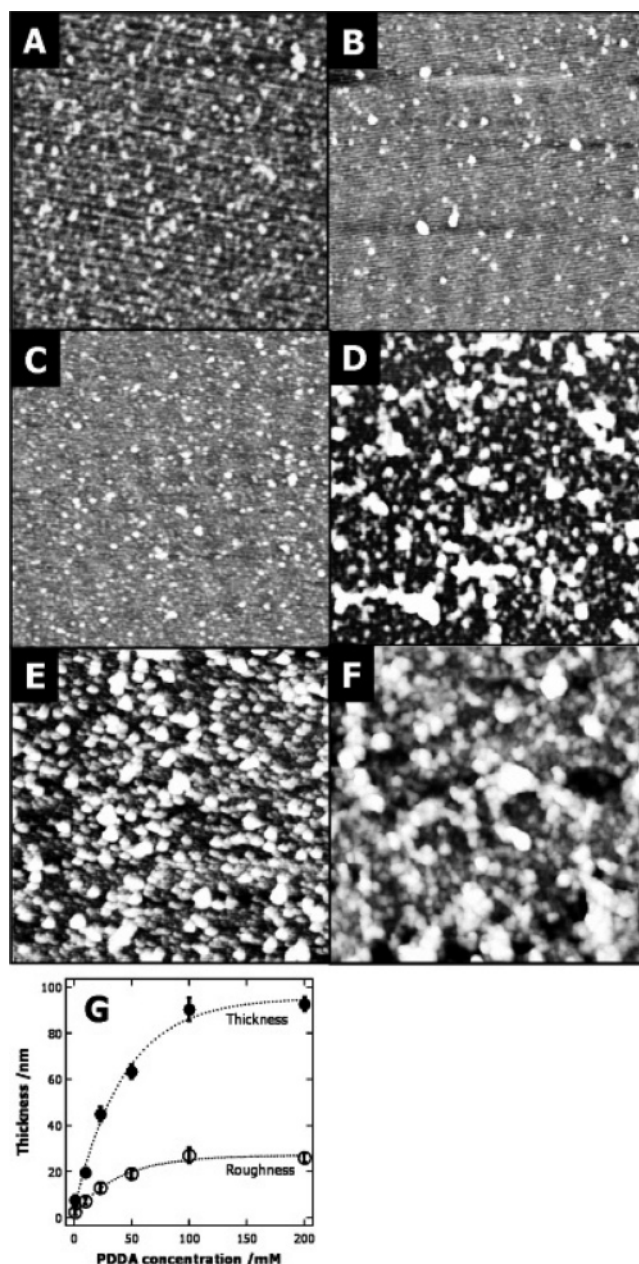


**Figure 5.** AFM height images of the 20-bilayer films. The film was deposited by the conventional LbL method with 1 mM/1 mM PAZO/PDDA for 90 s (A) and 30 min (B) of dipping time. The other AFM images are from the multilayer films deposited by the dynamic LbL methods with 1 mM PAZO and PDDA concentration of 1 mM (C), 10 mM (D), 50 mM (E), and 200 mM (F). The flow rates were set at 1 cm/s and the contact times were 90 s. All images are  $4 \times 4 \mu\text{m}^2$ . Depth scale is different as 10 nm (A, B, and C), 20 nm (D), 60 nm (E), and 100 nm (F). The film thickness and the rms roughness are shown in G.

ventional LbL method, a solution of higher ionic strength induces chain folding and increases the thickness, density, and the surface roughness of the film.<sup>7,9,10,35</sup> The pH is also pronounced because it affects the charge density of weak polyelectrolytes, but the relationship is somewhat complex.<sup>11–13</sup> In general, increasing the charge density of polyelectrolytes in solution induces chain extension, resulting in thinner and flat layers, whereas decreasing the charge density of polyelectrolyte produces thicker, loopy layers.<sup>11</sup>

**Adsorption Analysis.** The transport process in a homogeneous solution near a solid–liquid interface is governed by a subsurface layer through which diffusion

(34) Lowman, G. M.; Buratto, S. K. *Thin Solid Films* **2002**, *405*, 135.

(35) Kolarik, L.; Furlong, D. F.; Joy, H.; Struijk, C.; Rowe, R. *Langmuir* **1999**, *15*, 8265.

(36) Li, D. Q.; Lütt, M.; Fitzsimmons, M. R.; Synowicki, R.; Hawley, M. E.; Brown, G. W. *J. Am. Chem. Soc.* **1998**, *120*, 8797.

**Table 1. Constants Used to Fit the Experimental Adsorption Data<sup>a</sup>**

PDDA/mM	PAZO/mM	$K$	$\Gamma^\infty$
	0.05	$0.40 \pm 0.180$	$0.0050 \pm 0.0020$
	5	$0.04 \pm 0.005$	$0.0140 \pm 0.0010$
10		$1.68 \times 10^3 \pm 226$	$0.0040 \pm 0.0010$
25		$56.40 \pm 1.580$	$0.0065 \pm 0.0001$
200		$11.50 \pm 1.690$	$0.0140 \pm 0.0020$

<sup>a</sup>  $\pm 1$  standard deviation.

has to take place according to Fick's second law.<sup>37</sup> Diffusion of solutes occurs due to the concentration gradient between the bulk solution and the subsurface layer. Intensive studies on the various kinds of adsorption phenomena have been done.<sup>38–44</sup>

The Langmuir's classical treatment<sup>45</sup> is based on the equilibrium between the adsorption and desorption processes. The shape of the adsorbents is one of the factors that affects the equilibrium; for example, the lateral interaction between rigid particles influences the adsorption and desorption processes. The adsorption and desorption of flexible particles or polymers may require changes in their shape, structure, or conformation.<sup>46</sup> An additional complication often arises when the particles and the interface are charged. The transport of charged adsorbents is assumed to be at a local quasi-equilibrium within the subsurface layer when the formation of the subsurface layer is much faster than the characteristic time of adsorption.<sup>44,47</sup>

Even though our dynamic LbL method is not an equilibrium process, the adsorption data fit the Langmuir adsorption model very well, implying that the dynamic LbL method can be assumed to be at a quasi-equilibrium state. The data in Figure 4 are fitted with the Langmuir isotherm<sup>48,49</sup>

$$\Gamma = \frac{\Gamma^\infty KP}{1 + KP} \quad (1)$$

where  $\Gamma$  stands for the amount of adsorbed polymer,  $P$  is the polymer concentration,  $K$  is the adsorption constant, and  $\Gamma^\infty$  is the maximum amount of adsorbed polymer.<sup>45</sup> Table 1 lists the adsorption constant ( $K$ ) and the maximum adsorbed amount ( $\Gamma^\infty$ ) we obtained from the modeling.

The adsorption rate of PAZO was much higher than that of PDDA (at least 25 times). In other words, the concentration dependence of PAZO was much lower than that of PDDA. This difference is likely due to the difference in chain rigidity and the location of charge groups. The main chain of PDDA is more rigid than PAZO, and the charge groups are located on the main chain of PDDA versus on the side chains of PAZO. Therefore, the anionic groups of PAZO are more easily accessible for adsorption to a substrate. The data in Table 1 indicate that the

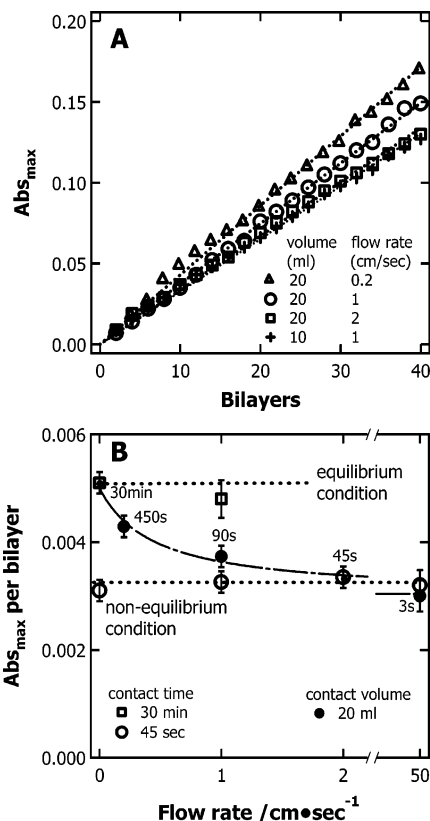


**Figure 6.** (A) Maximum UV/Vis absorption intensity at various flow rates of polyelectrolytes as the number of layers increases. The flow rates were 0.2 ( $\Delta$ ), 1 ( $\circ$ ), and 2 cm/s ( $\square$ ) for injecting 20 mL of solutions and 1 cm/s ( $+$ ) for injecting 10 mL of solutions. Cleaning the fluidic channel with 20 mL of deionized water was conducted at a flow rate of 1 cm/s to remove unbound polyelectrolytes. (B) The effect of contact time on the average UV/Vis absorption intensity ( $\lambda_{\text{max}} \sim 366$  nm) per bilayer. An equilibrium ( $\square$ ) and a nonequilibrium ( $\circ$ ) deposition condition were established by controlling the contact time of polyelectrolyte solutions at 30 min and 45 s, respectively. Intermediate data ( $\bullet$ ) between the dotted lines are from the experiment where the flow rate of 20 mL polyelectrolyte solutions changed from 3 to 450 s. The concentration of the polyelectrolyte pair was 1 mM/10 mM PAZO/PDDA. Zero flow rate experiments were done by conventional LbL dipping method. Dotted lines are guides for the eye.

adsorption from a more dilute solution reaches its equilibrium thickness (thinner, i.e., a smaller  $\Gamma^\infty$ ) faster (a larger  $K$ ) than from a more concentrated solution as we can intuitively expect.

To better understand the adsorption kinetics of our dynamic LbL system, we further analyzed the adsorption behavior. Figure 6A shows a linear increase of the UV/Vis absorption intensity along the layer deposition number. At a first glance, the amount of adsorbed polymer seems to increase as the flow rate decreases as shown in Figure 6A. However, it turned out that the contact time and not the flow rate actually affected the bilayer thickness. We confirmed this by conducting equal contact time experiments in two different regimes, an equilibrium condition and a nonequilibrium condition.

Conventional LbL deposition is done by dipping the substrate into the polyelectrolyte solution for at least 15 min, by which time 95% of the adsorption occurs, and the adsorption reaches its equilibrium at around 30 min.<sup>9,10,50</sup>

(50) Plech, A.; Salditt, T.; Münster, C.; Peisl, J. *J. Colloid Int. Sci.* **2000**, *223*, 74.

(37) Fick, A. *Ann. Phys. Chem.* **1855**, *94*, 59.  
 (38) Dukhin, S. S.; Kretzmar, G.; Miller, R. *Dynamics of Adsorption at Liquid Interfaces*; Elsevier: Amsterdam, Netherlands, 1995.  
 (39) Ward, A. H. F.; Tordai, L. *J. Phys. Chem.* **1946**, *14*, 453.  
 (40) Levich, V. G. *Physicochemical Hydrodynamics*; Prentice Hall: NJ, 1962.  
 (41) Probstein, R. F. *Physicochemical Hydrodynamics, An Introduction*; Butterworth: MA, 1989.  
 (42) Cohen Stuart, M. A.; Hoogendam, C. W.; de Keizer, A. *J. Phys.: Condens. Matter* **1997**, *9*, 7767.  
 (43) Avena, M. J.; Koopal, L. K. *Environ. Sci. Technol.* **1999**, *33*, 2739.  
 (44) Filipova, N. L. *J. Colloid Int. Sci.* **1999**, *211*, 336.  
 (45) Langmuir, I. *J. Am. Chem. Soc.* **1918**, *40*, 1361.  
 (46) De Gennes, P.-G. *Adv. Colloid Int. Sci.* **1987**, *27*, 189.  
 (47) Oyama, H. T.; Inoue, T. *Macromolecules* **2001**, *34*, 3331.  
 (48) Karpovich, D. S.; Blanchard, G. J. *Langmuir* **1994**, *10*, 3315.  
 (49) McKee, S.; Swailes, D. *J. Phys. A: Math. Gen.* **1991**, *24*, L207.

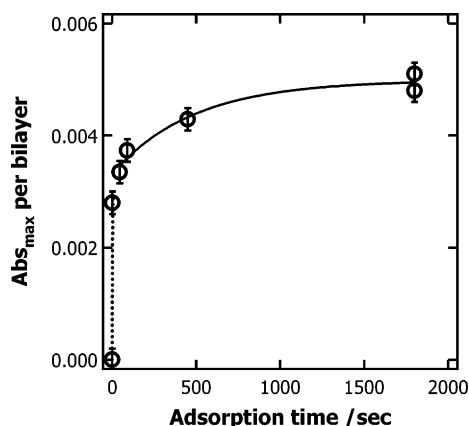


**Figure 7.** Average UV/Vis absorbance ( $\lambda_{\max} \sim 366$  nm) as the adsorption time increases. The concentrations of the polyelectrolytes were 1 mM/10 mM PAZO/PDDA. The dotted line and the solid line were fitted by using eq 2.

We prepared 20-bilayer films from 1mM/10mM PAZO/PDDA solutions with the conventional LbL method with a 30 min dipping time and with our dynamic LbL method with a 30 min contact time. As shown in Figure 6B (open squares), the UV/Vis absorption intensities per bilayer of the multilayer films from both methods are very close to each other.

For the equal contact time study in a nonequilibrium regime, we made 20-bilayer films from 1 mM/10 mM PAZO/PDDA solutions by using the conventional LbL method and our dynamic LbL method, for a constant contact time of 45 s by manipulating the solution volume and the flow rate (open circles in Figure 6B). Regardless of the flow rate, the amounts of adsorbed polyelectrolytes were the same as long as the contact time was maintained at a same value through the entire laminar flow regime—the Reynolds number ( $Re$ ) is around 7, 33, 66, and 1950 for 0.2, 1, 2, and 50 cm/s flow rate, respectively. Therefore, we conclude that the contact time not the flow rate is influential to the amount of adsorbed polyelectrolyte in the laminar flow regime. This conclusion is supported by the large adsorption constant ( $K = 1.68 \times 10^3$ ) of the 1 mM/10 mM PAZO/PDDA system. This large adsorption constant likely means a negligible desorption process within the applied flow rate range. Consequently, the amount of the adsorbed polyelectrolyte would be determined by the contact time.

The amounts of adsorbed polyelectrolytes per bilayer at differing contact times are shown as solid circles in Figure 6B. We controlled the contact time by adjusting the flow rate of 20 mL polyelectrolyte solutions. Even the shortest contact time of 3 s seems to be long enough for polyelectrolyte to adsorb onto the oppositely charged surface, which suggests the large adsorption constant  $K$  for this system.

Further adsorption kinetic analysis was conducted on the data in Figure 6 that were obtained from the different flow rate experiments. First, the data were manipulated in such a way that UV/Vis absorption intensities per bilayer were plotted versus the contact time as shown in Figure 7.

Filipova developed a kinetic model for adsorbing polyelectrolytes onto a planar surface under an external flow.<sup>44</sup> By following his mathematical framework, one could find the following relationship

$$t \sim \begin{cases} \Gamma, & (t \ll t_{\text{dif}}) \\ -\ln(1 - \Gamma), & (t \gg t_{\text{dif}}) \end{cases} \quad (2)$$

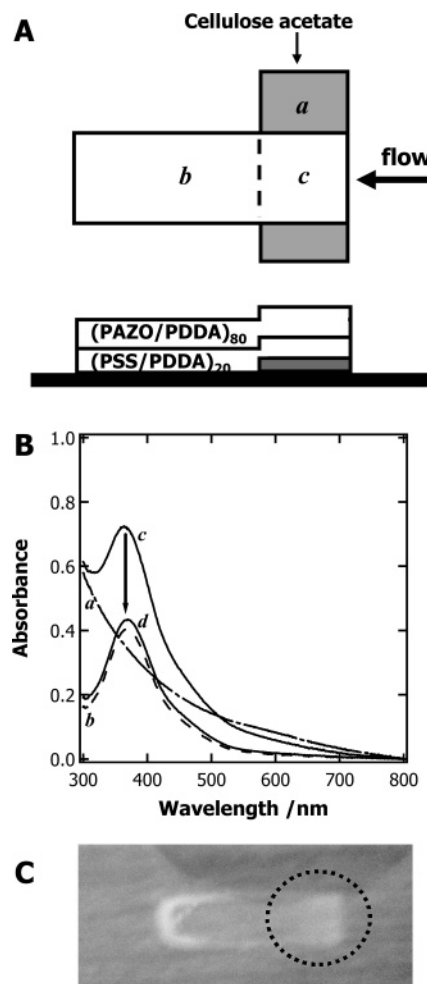


**Figure 8.** (A) Schematic view of the half-tethered self-standing film. (B) UV/Vis absorption spectra before and after removal of the sacrificial cellulose acetate layer. The characters ( $a$ ,  $b$ , and  $c$ ) represent the corresponding regions in A, where the UV/Vis spectra were recorded, and the  $d$  is the UV/Vis absorption spectrum after removal of the sacrificial layer of the region  $c$ . (C) The resulting half-tethered self-standing film. Self-standing region is inside the circle.

where  $\Gamma$  stands for the amount of adsorbed polymer,  $t$  is the adsorption time, and  $t_{\text{dif}}$  is the characteristic diffusion time of the polymer. In diffusion-controlled adsorption, the adsorbed amount usually depends on  $t^{1/2}$  rather than  $t$ ,<sup>39</sup> but the adsorption in this small time scale is beyond our experimental capability. For a longer time scale, a pseudo-first-order kinetic model is widely used to analyze the adsorption or a first-order reaction system.<sup>47,49,51</sup> Equation 2 holds true if the desorption process is negligible and the adsorption process is first order, which is our case. The data were fitted with eq 2 as shown in Figure 7. The convective diffusion seems to occur very fast in this system because the linear growth region in Figure 7 is within a very short period of time; therefore,  $t_{\text{dif}}$  is very small, possibly within a few seconds. All the data in the longer contact time regime agree very well with the exponential growth [see solid line fitted with  $\Gamma = 1 - \exp(-ckt)$ ], and the characteristic adsorption time ( $\tau$ ) is around 500 s. The characteristic time value further leads to the adsorption rate constant ( $k$ ) of  $\sim 2 \text{ L mol}^{-1} \text{ s}^{-1}$  taking into account that 1 mM PAZO adsorbs onto the oppositely charged PDDA surface. From this kinetic analysis, the following information could be deduced. The first adsorp-

tion process starts within seconds of exposure of the charged surface to the polyelectrolyte solution, followed by a slower growth regime, where both thickness and density change over a range of about 10 min. This interpretation agrees very well with the results by Plech et al.<sup>50</sup>

**Self-Standing Film Fabrication.** The LbL self-assembly technique has been used to create and integrate nanostructured composites into devices.<sup>14</sup> For this purpose, a lithographic technique can be combined with the LbL self-assembly. However, this requires time-consuming multistep fabrication processes. Alternatively, the nanocomposite prepared by the LbL method can be detached from a substrate and deposited onto other substrates. In this case, however, the final shape and orientation of the resulting self-standing nanocomposite are beyond experimental control.<sup>52</sup>

Here, we present a much simpler, yet effective method to build a self-standing film to demonstrate the facile and region-selective coating capability of our dynamic LbL sequential deposition method. Figure 8A shows a schematic view of the fabricated film on a substrate. The glass substrate was predeposited with PDDA to render positive charges on the surface. Cellulose acetate (slight negative charge)<sup>52</sup> was first mixed with methylene blue and then dip-coated onto the positively charged glass surface; methylene blue was used to characterize the film by UV/Vis spectroscopy. The LbL multilayer film was then constructed on the cellulose acetate layer by using our dynamic sequential LbL method with a 10 mM/10 mM PSS/PDDA pair and a 1 mM/10 mM PAZO/PDDA pair as depicted in Figure 8A. After the film was air dried, cellulose acetate was selectively dissolved in acetone to release the half-tethered self-standing film. UV/Vis absorption spectra of each region of the film before and after the cellulose acetate removal are shown in Figure 8B. The UV absorption spectra *a*, *b*, and *c* were taken on the cellulose acetate only region, the LbL film only region, and the area of both the cellulose acetate and the LbL film, respectively. The spectrum *d* was taken on the same area as in *c* after dissolving the cellulose acetate. After the sacrificial cellulose acetate layer was removed, the final UV spectrum (*d*) became almost identical to *b*, confirming completely selective removal of the sacrificial cellulose acetate layer. The picture of the resulting film is shown in Figure 8C.

(52) Mamedov, A. A.; Kotov, N. A. *Langmuir* **2000**, *16*, 5530.

Inside of dotted circle, a slight decrease in the refractivity of the film was observed.

By using our dynamic deposition method, we successfully constructed a region-selective half-tethered self-standing multilayer film with a simple three-step process. This new dynamic LbL method has a potential capability to align rigid-rodlike conjugated polymers. We are currently investigating the shear effect of the dynamic LbL method on the degree of alignment of rodlike polyelectrolytes polymers.<sup>53</sup>

## Conclusions

We have devised a dynamic sequential LbL deposition method to deposit well-defined multilayer polyelectrolyte films on a substrate. This newly developed method enables us to fabricate region-selective polymer coatings of desired shapes faster, and the resulting film quality is comparable to those from the conventional LbL method. The thickness of the film could be well-controlled by the number of injections, the concentration of polyelectrolyte solutions, and the duration of contact time. Surface roughness of the film prepared by the dynamic LbL method for 90 s of contact time was slightly larger than that from the conventional LbL method for 30 min of dipping time but still smaller than that from the conventional LbL method for the same 90 s of dipping time. The surface roughness increased as the concentration of polyelectrolyte solution increased. Our study on the adsorption analysis showed that the dynamic LbL deposition process follows the quasi-equilibrium Langmuir adsorption, and the key control is the contact time in the electrostatic adsorption process. We demonstrated the simplicity and the region-selective coating capability of this newly devised method by constructing a half-tethered self-standing multilayer film in three simple steps.

**Acknowledgment.** The authors appreciate the financial support of the UM College of Engineering start-up fund, the UM Rackham grant from the Horace H. Rackham School of Graduate Studies, and the National Science Foundation (BES 0428010).

LA0511182

(53) Our preliminary results showed promising main-chain alignment of poly(*p*-phenylene ethynylene) (PPE) electrolytes along the shear direction. The absorption intensity of monolayer films of PPE parallel to the shear direction is 3 times stronger than that of films perpendicular to the shear direction.